Supplementary Figure S1

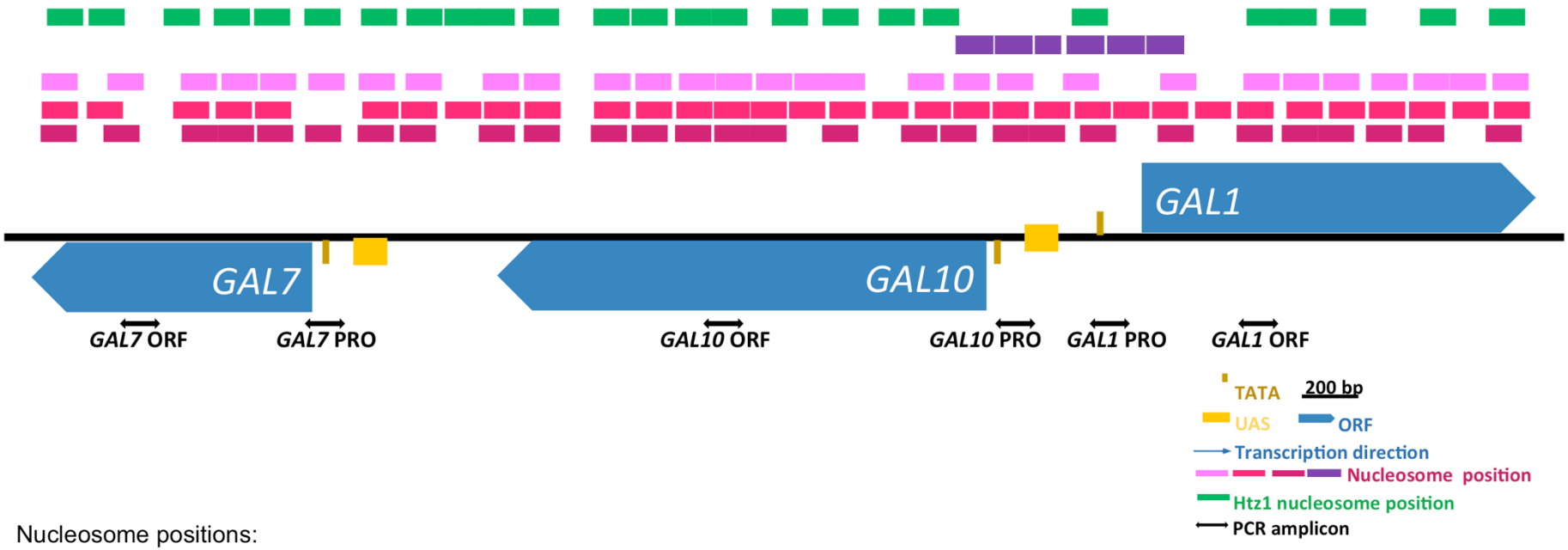

Nucleosome positions:

Mavrich et al 2007, A barrier nucleosome model for statistical positioning of nucleosomes throughout the yeast genome.

Lee et al 2007, A high-resolution atlas of nucleosome occupancy in yeast.

Jiang et al 2009, A compiled and systematic reference map of nucleosome positions across the *Saccharomyces cerevisiae* genome

Floer et al 2010, A RSC/nucleosome complex determines chromatin architecture and facilitates activator binding

Htz1 positions:

Albert et al 2007, Translational and rotational settings of H2A.Z nucleosomes across the Saccharomyces cerevisiae genome.

Figure S1. Schematic of the *GAL* locus. Positions (black lines with arrows) of the quantitative real-time PCR fragments indicating the promoter (PRO) and open reading frame (ORF) regions of the *GAL7, GAL10* and *GAL1* genes (open reading frames indicated by blue filled arrows). Nucleosome mapping information from a variety of studies is indicated.

Supplementary Figure S2

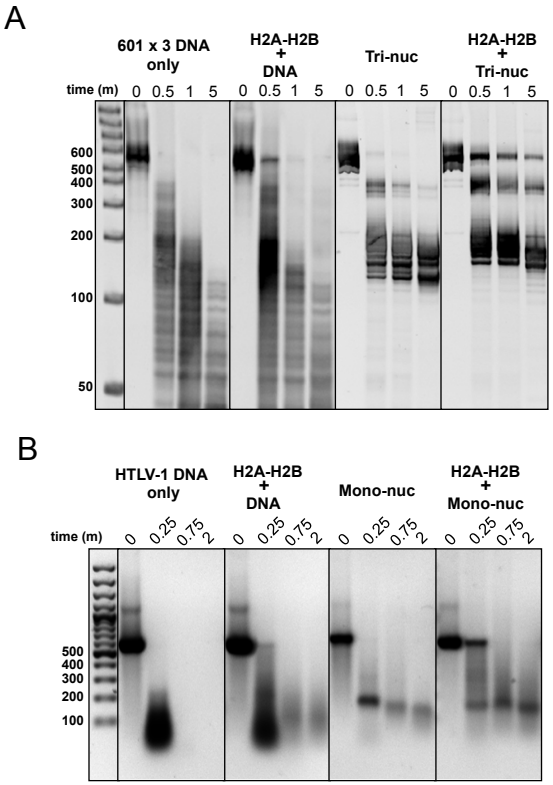

Figure S2. H2A-H2B accumulation protects DNA from MNase digestion. Analyses of MNase digestion of A) a 621 bp 601 (601 x 3) DNA fragment capable of forming tri-nucleosomes, composed of three consecutive 207 bp Widom 601 nucleosome positioning sequences with linker DNA, and B) a 588 bp HTLV-1 LTR DNA fragment capable of forming mono-nucleosome. MNase digestion of naked DNA alone (first panels), DNA with H2A-H2B (second panels), chromatin (third panels), and chromatin with excess H2A-H2B (fourth panels).

Supplementary Figure S3

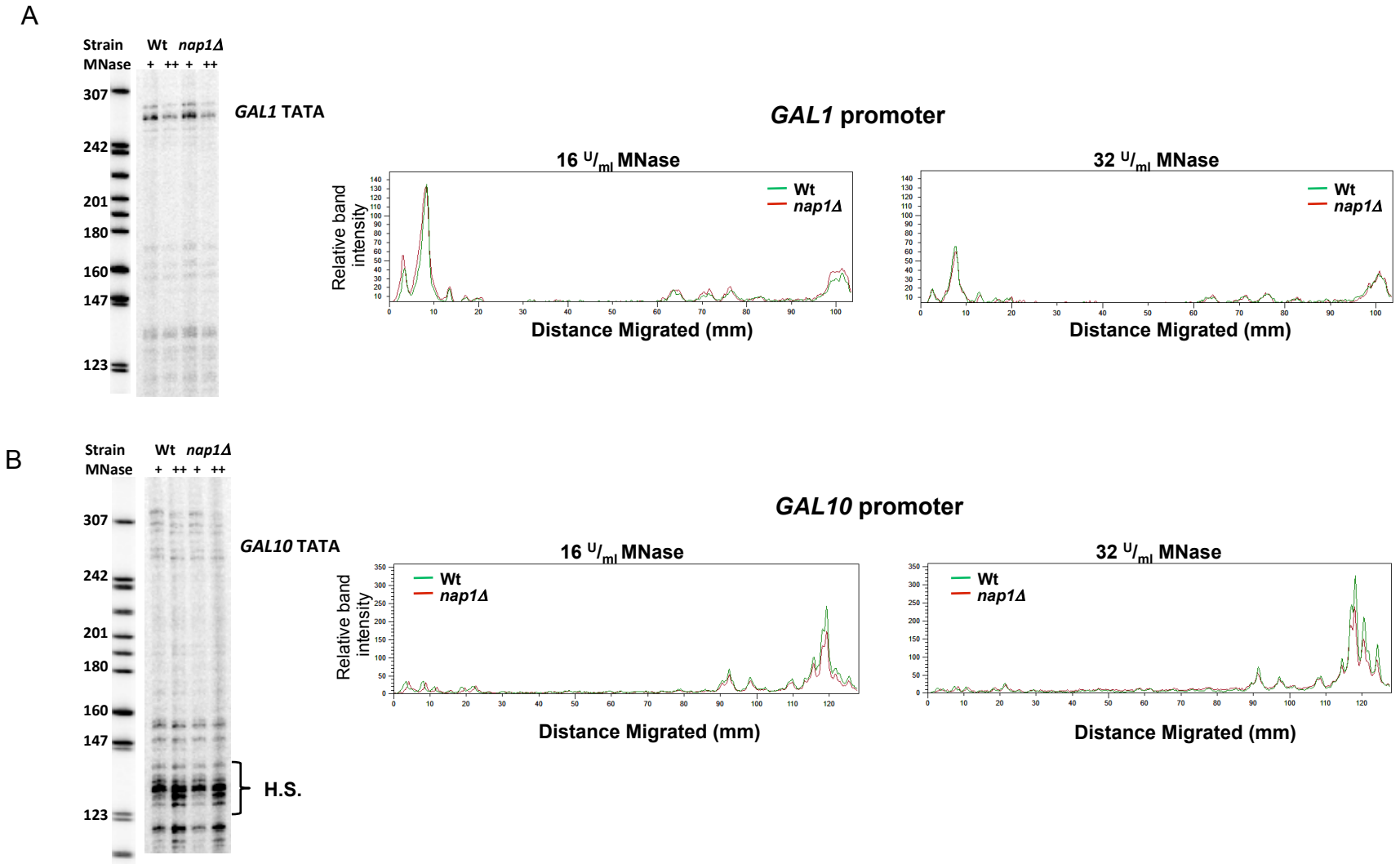

Figure S3. The binding of excess H2A-H2B to the *GAL10* promoter does not grossly affect chromatin architecture, but does partially occludes MNase cleavage. A) Phosphor-image and quantitation of extension products from the *GAL1* promoter region and chromatin from wild type (green) or *nap1Δ* cells (red). This region of the *GAL* locus does not accumulate excess dimer when *NAP1* is deleted. B) Phosphor-image and quantitation of extension products from the *GAL10* promoter region and chromatin from wild type (green) or *nap1Δ* cells (red). This region of the *GAL* locus accumulates excess dimer when *NAP1* is deleted. Radio-labeled DNA size standards and lengths are shown to the left of each gel image. The location of the *GAL1* and *GAL10* TATA sequences and the MNase hyper-sensitive sites (HS) adjacent to the UAS are indicated to the right of each gel image. The + and ++ above the lanes correspond to, 16 or 32 $^{U}/_{ml}$ of MNase, respectively used to digest each sample.

Supplementary Figure S4

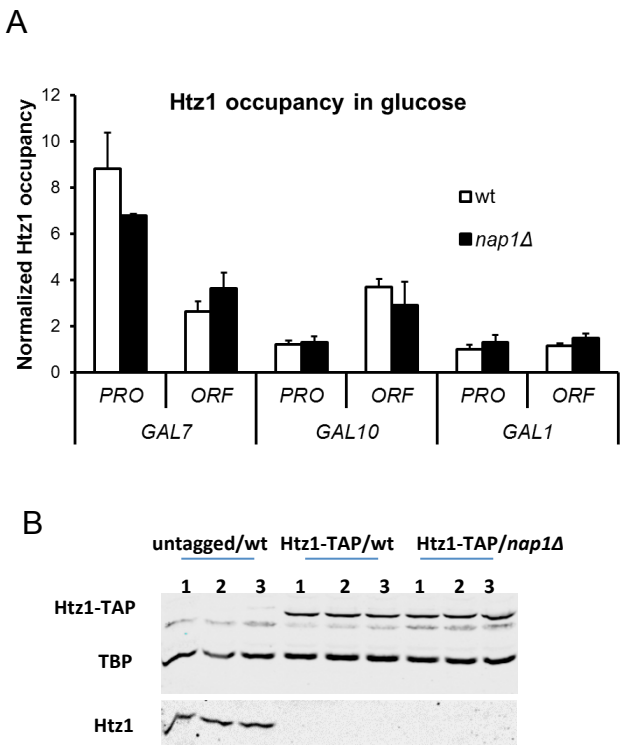

Figure S4. Occupancy of the histone variant H2A.Z (Htz1) is unchanged in the *nap1Δ* strain A) Occupancy of TAP tagged Htz1/H2A.Z at the *GAL* locus in the wild type (white bars) and nap1Δ (black bars) strain via chromatin-tandem affinity purification assay. Occupancy at each *GAL* location was normalized to occupancy at the telomere. Bars reflect the means of three biological replicates ± standard deviation; no significant differences were observed. B) Western blots of Htz1 levels in wild type (wt) and *nap1Δ* cells indicate no change in levels; TBP levels are shown as an internal control.

Supplementary Figure S5

A

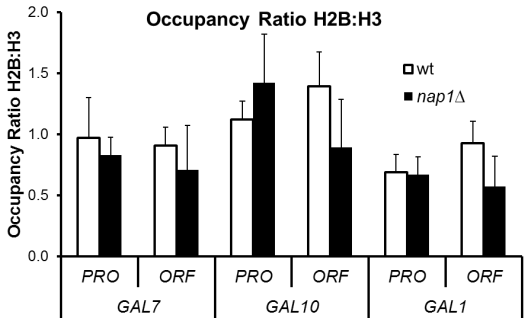

B

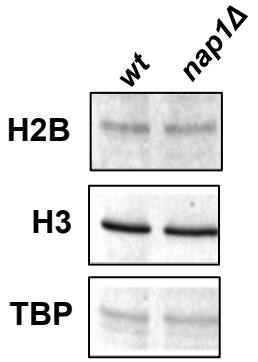

Figure S5. When induced, the *GAL* locus does not accumulate H2A-H2B in *nap1Δ*. A) Ratios of H2B to H3 occupancy at the *GAL* locus when cells are cultured in galactose (activated condition) show no differences between the wild type (white bars) and *nap1Δ* (black bars) strains. The histone occupancy of H2B and H3 were determined by ChIP assays. B) Western blots of total histone levels in wt and *nap1Δ* cells cultured in galactose indicate no change in levels; TBP levels are shown as an internal control.

Supplementary Figure S6

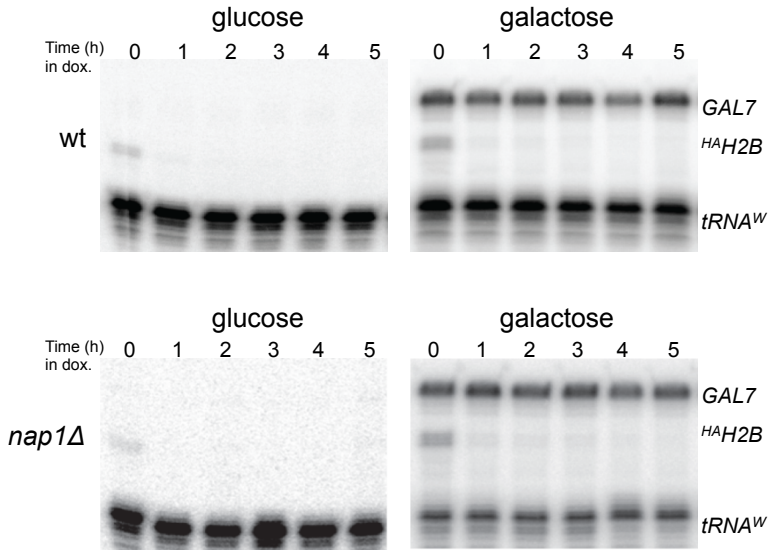

Figure S6. Doxycycline represses HA-tagged histone mRNA expression and does not affect *GAL* gene expression. The wild type and *nap1*Δ strains were cultured under transcriptionally repressed (glucose) or active (galactose) conditions. After the addition of doxycycline, cells were collected every hour for five hours. Total RNA was isolated from each sample and ^{HA}*H2B*, *GAL7* and *tRNA*^{W} transcripts were detected by S1 nuclease digestion using a ^{32}P-labeled probe specific to ^{HA}*H2B*, *GAL7* or *tRNA*^{W}. The transcript level of the doxycycline-regulated HA-tagged histone diminishes within one hour of doxycycline treatment in both glucose and galactose media.

Supplementary Figure S7

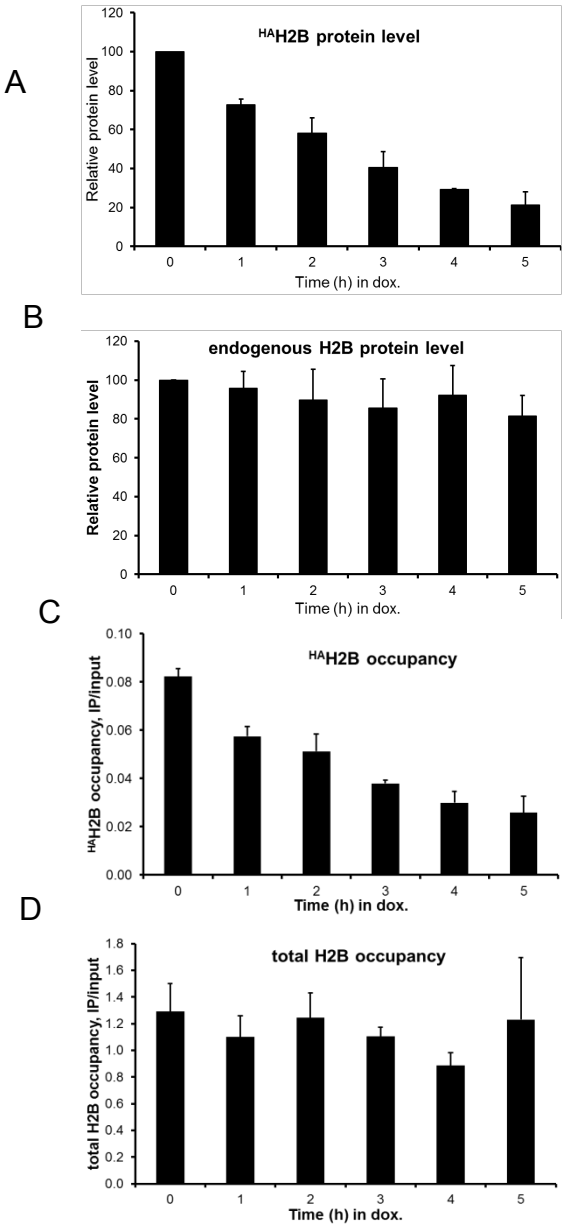

Figure S7. ^{HA}H2B protein level and chromatin occupancy at a telomere-proximal region decrease during treatment. The wild type strain containing both endogenous histone H2B and doxycycline-regulated histone ^{HA}H2B (plasmid-born, HA-tagged) was cultured under transcriptionally repressed conditions. Following addition of doxycycline (to turn off expression of ^{HA}H2B), cells were collected every hour for 5 hours, followed by immunoblotting to determine protein expression level and ChIP to determine occupancy. The HA-tagged histones represent less than 1% of the total (tagged and endogenous) histone expression levels (data not shown), therefore assays utilizing an anti-H2B antibody reflect primarily the endogenous protein. A) The protein levels of tagged histone ^{HA}H2B were detected using anti-HA antibody. B) The protein levels of endogenous histone H2B were detected using anti-H2B antibody. The occupancy of tagged histone ^{HA}H2B (C) and endogenous histone H2B (D) at a telomere proximal location during doxycycline treatment was determined by ChIP assay. The protein expression level and occupancy of the doxycycline-regulated histone ^{HA}H2B drops temporally following doxycycline treatment whereas the endogenous histone level and occupancy does not. Data in (A)-(D) reflect the mean from 3 biological replicates ± standard deviation.

Supplementary Figure S8

A

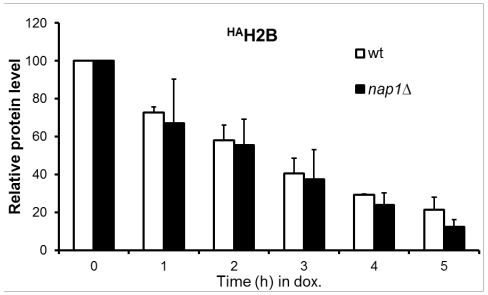

B

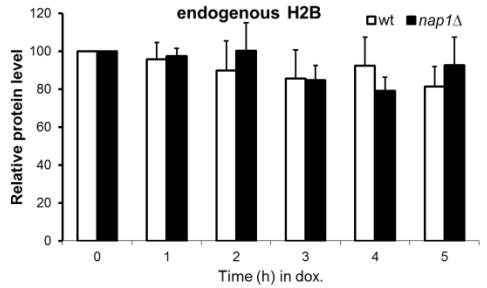

C

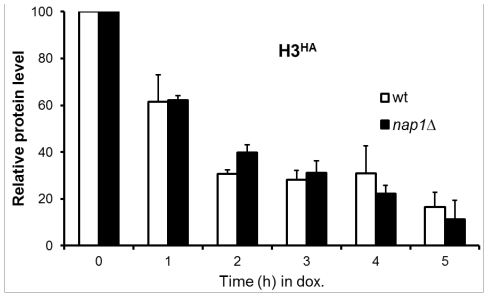

D

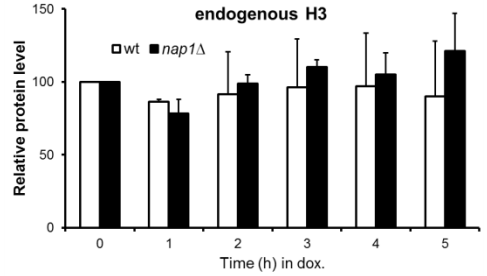

Figure S8. The cellular protein levels of ectopically expressed HA-tagged histones and endogenous histones are not affected by the deletion of Nap1. The wild type strain (shown in white) and the *nap1*Δ strain (shown in black), both containing endogenous histones and the plasmid expressing doxycycline-regulated HA-tagged histone (^{HA}H2B or H3^{HA}), were cultured under transcriptionally repressed conditions (glucose). Following addition of doxycycline (to turn off the expression of ^{HA}H2B or H3^{HA}), cells were collected every hour for 5 hours, followed by immunoblotting. The HA-tagged histones represent less than 1% of the total (tagged and endogenous) histone expression levels (data not shown), therefore assays utilizing an anti-H2B or anti-H3 antibody reflect primarily the endogenous protein. The protein expression levels of ^{HA}H2B (A) and H3^{HA} (B) were detected with anti-HA antibody. The protein expression levels of the total/ endogenous H2B (C) and H3 (D) were detected with anti-H2B and anti-H3 antibodies, respectively. The protein expression level (for HA-tagged or endogenous histones) at T_0 in each strain was set as 100. Bars reflect the means of three biological replicates ± standard deviation.

Supplementary Figure S9

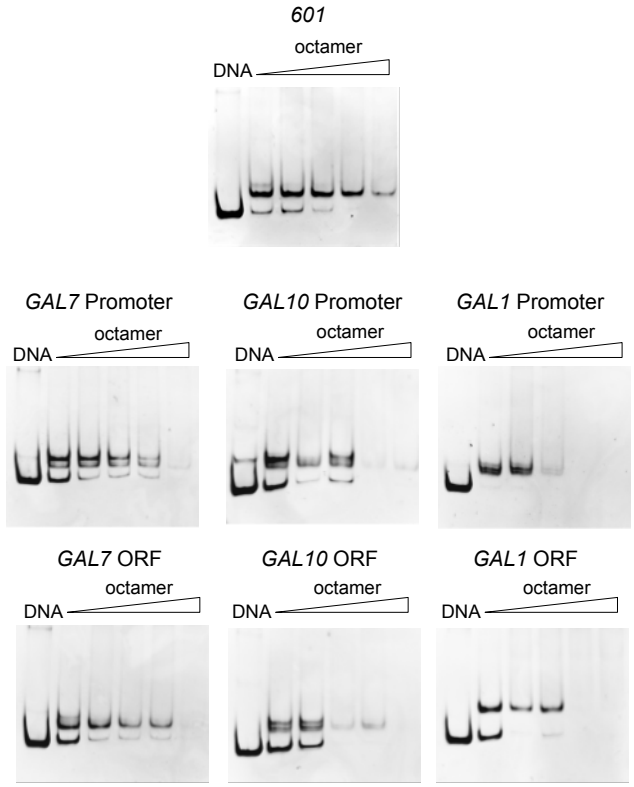

Figure S9. DNA sequence affects nucleosome formation and stability. Nucleosome reconstitutions with 601, and the indicated *GAL* fragments. Increasing molar amounts of histone octamer were incubated with the indicated DNA fragments, complexes were resolved in 5% native gels and DNA visualized by ethidium bromide staining.

Supplementary Figure S10

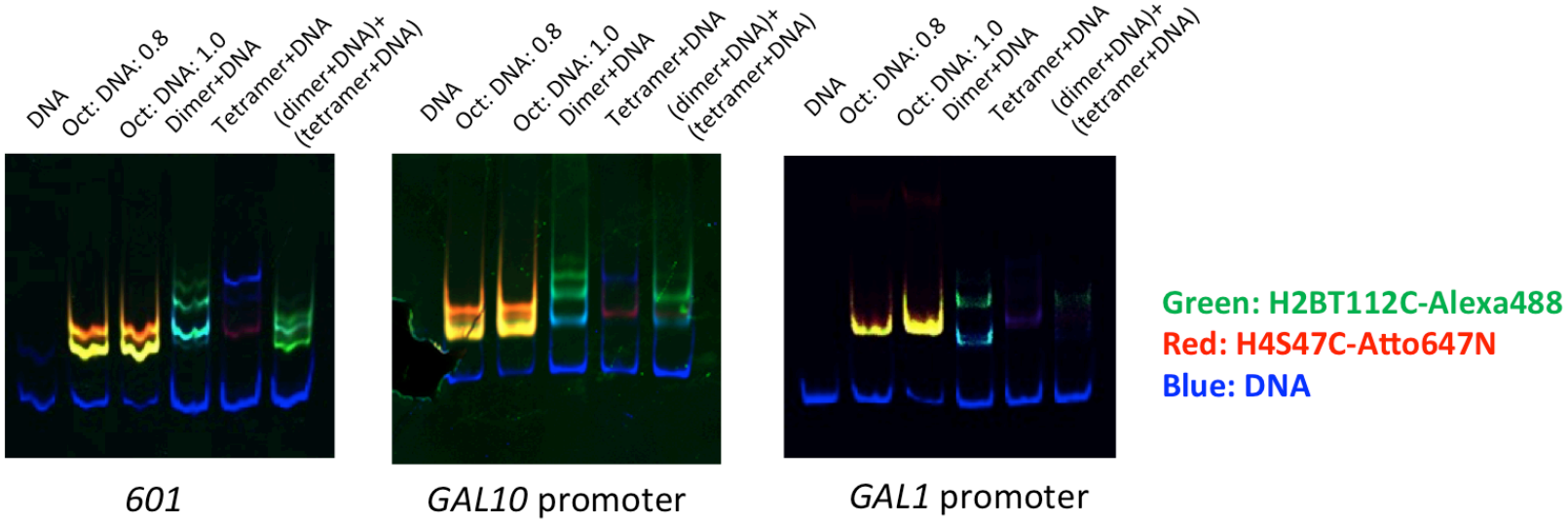

Figure S10. Hexasome and nucleosome formation is dependent upon DNA sequences. In the nucleosome reconstitution with histone octamer and DNA fragments using salt dilution method (as shown in Supplemental Figure 9) multiple forms of DNA-histone complexes were detected. To identify the complexes, nucleosome reconstitution was performed with fluorescently labeled histones. The Alexa488 labeled H2B is shown in green and Atto647N labeled H4 in red. Therefore, the canonical nucleosome with equal molar of H2B and H4 would be visualized in yellow and the hexasome with H2B to H4 ratio as 1:2 would be in orange. Representative gels of 601, the *GAL10* promoter (GAL10PRO) and *GAL1* promoter (GAL1PRO) are shown. Based on the color and intensity, we conclude both hexasome and nucleosome are formed on 601 and GAL10PRO. In contrast GAL1PRO forms predominantly nucleosomes.

Supplementary Figure S11

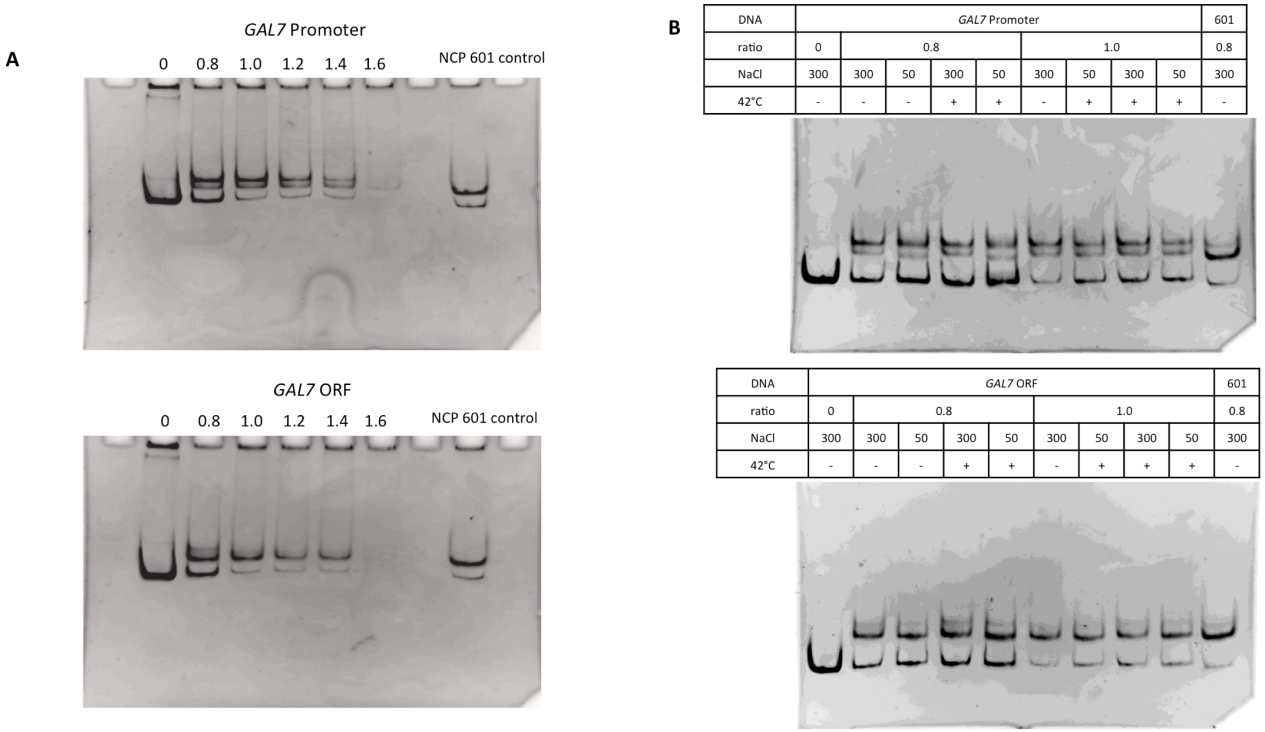

DNA	GAL7 Promoter									601
ratio	0	0.8				1.0				0.8
NaCl	300	300	50	300	50	300	50	300	50	300
42°C	-	-	-	+	+	-	+	+	+	-

DNA	GAL7 ORF									601
ratio	0	0.8				1.0				0.8
NaCl	300	300	50	300	50	300	50	300	50	300
42°C	-	-	-	+	+	-	+	+	+	-

Figure S11. Hexasome and nucleosome are stably position on the DNA sequences. It is possible that the multiple forms of DNA-histone complexes could be differently positioned nucleosomes. To test this, we incubated the reconstituted nucleosomes under different conditions, such as heat shift at 42°C, lower salt concentration (from 300 mM to 50 mM) or both, which would serve to disrupt non-positioned histone-DNA complexes. Representative gels for GAL7 promoter and ORF are shown. The results indicate that the pattern of DNA-histone complex bands does not change under these conditions, supporting the conclusion that these are stably positioned DNA-histone complexes.

Figure S12. Nap1 plays multiple roles in histone dynamics in vivo.

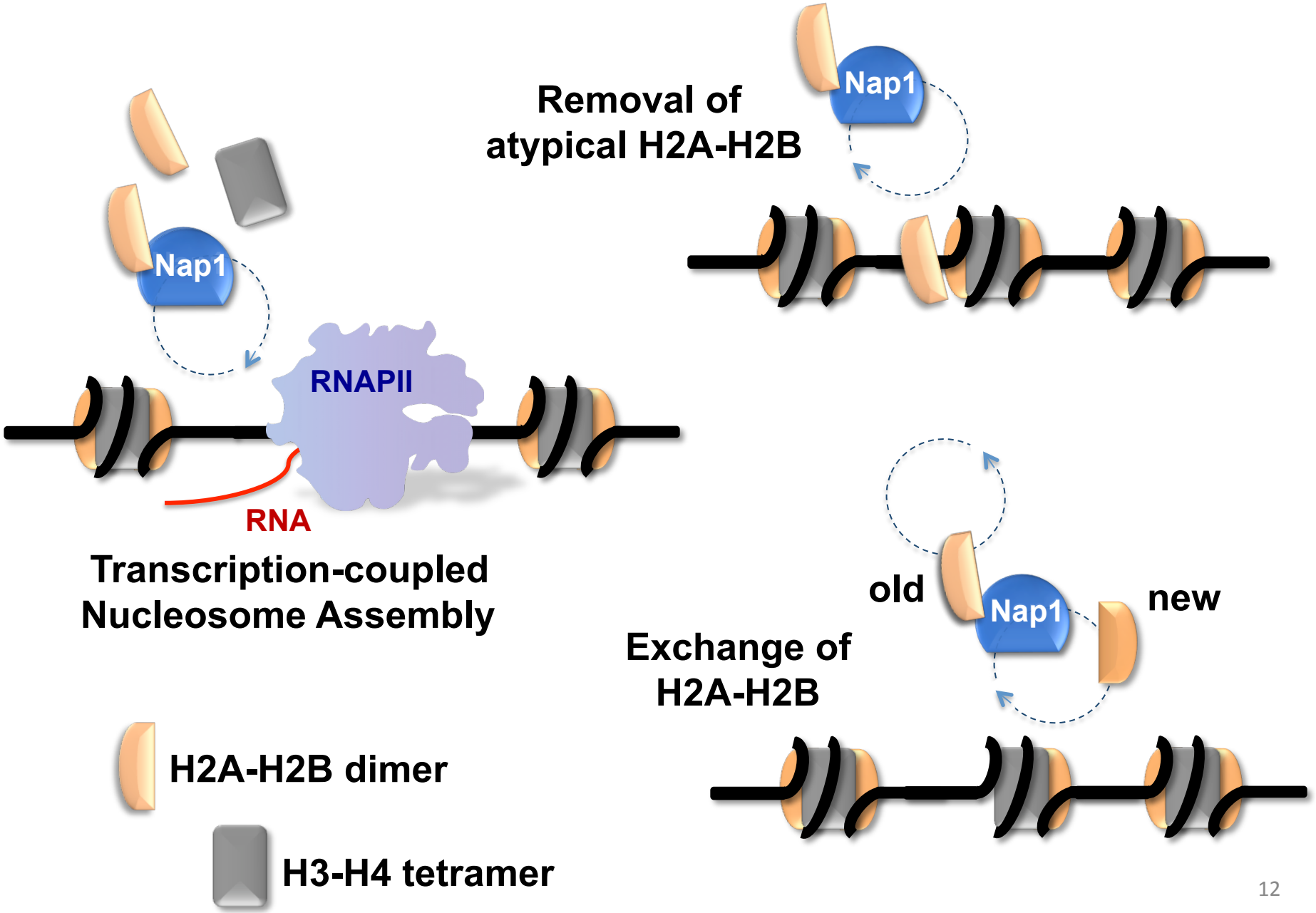

Supplementary Materials and Methods (Chen et al., 2015)

Isolation of yeast nuclei and MNase digestion: Nuclei were isolated from wild type (BY4741) and *nap1Δ* cells essentially as described (1). Wild type and *nap1*Δ cells were grown in YPD at 28°C to an OD_{600} of approximately 1.0. Formaldehyde was added to each culture to yield a final concentration of 1%. The cultures were incubated at room temperature with mixing every five minutes for a total of 15 minutes. Cross-linking was then quenched by the addition of glycine to a final concentration of 0.35M. The cultures were incubated an additional 5 minutes at room temperature and the cells collected by centrifugation. The cell pellets were washed two times with 30 mls of Sorbitol buffer (50 mM Tris-Cl pH 7.5, 1.0 M Sorbitol, 10 mM $MgCl_2$, 10 mM β-Mercaptoethanol, 1mM PMSF), the pellets weighed and suspended in 0.66 ml Sorbitol buffer per gram of cells. The cell suspensions were incubated at 30°C for 10 minutes with gentle agitation. 0.34 ml of Zymolase (10 $^{mg}/_{ml}$) per gram of cells was added to each of the cell suspensions and the samples incubated at 30°C with gentle agitation. Spheroplast formation was monitored after 15 minutes by combining 4 µl of cell suspension with or without Zymolase, 4 µl 10 % SDS and 992 µl of ddH_2O, mixing and determining the OD_{600} of the samples. When the OD_{600} of the sample with Zymolase was approximately 10 % of the sample without Zymolase, the Spheroplast suspension was diluted to 30 ml by slowly adding sorbitol buffer and the spheroplasts collected by centrifugation. The spheroplasts were washed two times with 30 ml of Sorbitol buffer and gently suspended in 20 ml of Ficoll buffer (20 mM Tris-Cl pH 7.5, 18% Ficoll 400, 0.5 mM $MgCl_2$). The spheroplast suspension was transferred to a chilled Potter-Elvehjem homgenizer, the pestle attached to a hand-held drill and the suspension homogenized on ice by 6-8 strokes at max rpm. The homogenate was transferred to a chilled 25 ml centrifuge tube and remaining cells pelleted by centrifugation. The supernatant above the cell pellet was carefully pulled off

and transferred to a chilled 25 ml centrifuge tube. Nuclei were collected by centrifugation and the supernatant pulled off and discarded. The crude nuclei pellet was suspended in 10 ml of MNase digestion buffer (20 mM Tris-Cl pH 8.0, 1.5 mM $CaCl_2$, 150 mM NaCl, 1 mM PMSF), 10 µl of the suspension removed, diluted to 1 ml with digestion buffer and the OD_{600} determined. The nuclei were collected by centrifugation and suspended in 2.4 ml of digestion buffer per 0.2 OD_{600}. 400 µl aliquots of the nuclei suspension were transferred to 1.7 ml centrifuge tubes and the samples incubated at 37°C for 10 minutes. While the samples were incubating six dilutions of MNase (Worthington Biochemical, 10 $^{U}/_{ml}$) were prepared. 4 µl of each MNase dilution were added to the nuclei suspensions, the samples mixed and incubated at 37°C for an additional 10 minutes. The final MNase concentrations were 1, 2, 4, 8, 16 and 32 $^{U}/_{ml}$. The MNase digestions were stopped by the addition of 100 µl of stop solution (140 mM EDTA, 3.5% SDS, 0.35 $^{mg}/_{ml}$ Proteinase K). The samples incubated at 37°C for one hour and the formaldehyde crosslinking reversed by incubation overnight at 65°C. The samples were extracted two times with phenol/chloroform and one time with chloroform, and ethanol precipitated. The DNA was suspended in 100 µl of T.E. pH7.5, 1 µl of RNaseA (10 $^{mg}/_{ml}$) added and the samples incubated at 37°C for 30 minutes. The DNA was ethanol precipitated and suspended in 100 µl of T.E. pH7.5.

Indirect end-labeling analysis: 15 µl aliquots of the wild type and *nap1Δ* DNA samples digested with 0, 16 and 32 $^{U}/_{ml}$ of MNase were cleaved by EcoRV, electrophoresed through a 1.5 % Agarose-TBE gel and the DNA transferred from the gel to a nylon membrane using a standard capillary transfer. A 395 bp EcoRV-Apa1 DNA fragment from the *GAL1* gene was labeled with ^{32}P using a Random Primer DNA Labeling Kit (TaKaRa Bio Incorporated) and hybridized to the membrane bound DNA using standard procedures (2).

Reiterative primer extension analysis: The wild type and *nap1Δ* DNA samples digested with 16 and 32 U/ml of MNase were purified by passage through Sephadex G-50 column. Oligonucleotides complimentary to the *GAL1-10* UAS and *GAL1* gene were labeled with ^{32}P using T4 polynucleotide and $^{\gamma 32}P$-ATP. 10 µl of the DNA samples digested with MNase were combined with 0.5 pmol of labeled primer, 4µl of 5X Taq buffer, 2 µl 2.5 mM dNTPs and water to yield a final volume of 20 µl. The samples were placed on ice and 5 µl of Taq polymerase (1U/µl in 1X Taq buffer) added to each, the samples mixed and spun briefly. The samples were placed in a thermocycler and the following profile repeated 20 times: 30 seconds at 95^{o}C, 30 seconds at 55^{o}C, and 1.5 minutes at 68^{o}C. The reactions were transferred to 1.7 ml tubes and the DNA ethanol precipitated overnight at -20^{o}C. The DNA was pelleted by centrifugation, the pellets washed with 75%, dried and suspended in 5 µl of formamide loading dye. The DNA samples were incubated at 95^{o}C for 4 minutes, quick chilled on ice and 4 µl of each loaded onto a denaturing 6% polyacrylamide/TBE gel. The DNA was electrophoresed through the gel at 23 amps, the gel transferred to blotting paper and dried under vacuum.

In vitro MNase digestion with HTLV1-LTR Native, non-positioned nucleosomes were assembled into chromatin by salt dialysis using purified recombinant *Xenopus laevis* histone octamer at 2:7 mass ratio of octamer:DNA on a 588 bp HTLV-1 LTR DNA fragment (3). A 140 µl reaction mixture containing 25 µg DNA and the indicated amount of octamer were incubated in high salt buffer (2M NaCl, 10mM Tris pH7.5, 1mM EDTA, 0.1% CHAPS) for 20 min on ice and then subjected to dialysis (8 kDa cutoff dialysis membrane) in which high salt buffer was gradually exchanged with low salt buffer (50 mM NaCl, 10 mM Tris pH 7.5, 1 mM EDTA, 0.05% NP40, 4 mM 2-mercaptoethanol) in a constant volume of 400 ml for ~16 hrs at 4°C. Sample was then dialyzed for 3 hours at

4°C against low salt buffer containing 20% glycerol and stored at 4°C. Excess recombinant *Xenopus laevis* H2A/H2B was incubated at RT for 30 min in the presence of 5.5 µg 588bp HTLV-1 LTR DNA fragment unassembled or assembled into chromatin as indicated at a 6:1 mole ratio of dimer to octamer in a final reaction volume of 35 µl containing 50 mM NaCl, 10 mM Tris pH 7.5, 1 mM EDTA, 0.05% NP40, and 4 mM 2-mercaptoethanol. For micrococcal nuclease digestion, reaction mixtures (40 µl) were prepared by incubating 5.5 µg of the 588bp LTR fragment (either free in solution or assembled into chromatin and/or incubated with H2A/H2B dimer as indicated) in 20 mM Tris pH 8.0, 5 mM NaCl, 2.5 mM fresh $CaCl_2$ for 5 min at 37°C. Micrococcal nuclease (Takara; 1 unit per 1.25 µg DNA) was then added and a portion of each reaction (1.25 ug DNA) was removed at the indicated time during incubation at 37°C. Digestion was stopped by addition of 0.4 volumes of a solution containing 5 mM Tris pH 7.5 and 250 mM EDTA and samples were subjected to Proteinase K digestion (Thermo-Fisher) at 37°C for 1h in buffer containing 250 mM NaCl, 1% SDS, 20mM Tris pH7.5, and 5 mM EDTA. Samples were then phenol-chloroform extracted, ethanol precipitated, and analyzed by 1.5% agarose gel electrophoresis followed by ethidium bromide staining.

Immunoblotting of the soluble protein level

Cells were collected, resuspended in lysis buffer (Tris-phosphate pH 7.5) and lysed by vigorous bead-beating. The insoluble cell debris was removed by centrifugation. Equal amounts of soluble protein from each sample were subjected to 15% SDS/PAGE analysis and then transferred onto nitrocellulose membranes. The same antibodies against HA, H2B, and H3 that were used for ChIP analysis were used for protein detection.

Chromatin tandem affinity purification of Htz1-TAP

Cells were cultured in YP-glucose to mid-log phase. After cross-linking with formaldehyde, cells were spheroplasted with Zymolyase 20T in buffer containing 50mM Tris.Cl, pH7.5, 1.0 M sorbitol, 1mM MgCl2, 10mM β-mercaptoethanol. Spheroplasted cells were then lysed with FA lysis buffer (50mM Hepes/KOH, pH7.5, 140mM NaCl, 1mM EDTA, 1% Triton X-100, 0.1% Na Deoxycholate), and the insoluble material was sonicated using bioruptor UCD-200. Sheared chromatin material was pre-cleared with sepharose CL-4B for 1h at 4°C and the supernatant was then incubated with IgG sepharose 6 fast flow (GE, cat. #17-0969-01) overnight at 4^{o}C. Protein–DNA cross-links were reversed by incubation at 65°C, and the DNA was purified by phenol-chloroform extraction and used for quantitative PCR analysis.

References:

1. **Reese JC, Zhang H, Zhang Z.** 2008. Isolation of highly purified yeast nuclei for nuclease mapping of chromatin structure. Methods in molecular biology **463:**43-53.

2. **Ausubel FM.** 1987. Current protocols in molecular biology. Greene Pub. Associates;J. Wiley, order fulfillment, Brooklyn, N.Y. Media, Pa.

3. Geiger TR, Sharma N, Kim YM, Nyborg JK. 2008. The human T-cell leukemia virus type 1 tax protein confers CBP/p300 recruitment and transcriptional activation properties to phosphorylated CREB. Molecular and Cellular Biology **28:**1383-1392.

Supplemental Figure legends

Figure S1. Schematic of the *GAL* locus. Positions (black lines with arrows) of the quantitative real-time PCR fragments indicating the promoter (PRO) and open reading

frame (ORF) regions of the *GAL7, GAL10* and *GAL1* genes (open reading frames indicated by blue filled arrows). Nucleosome mapping information from a variety of studies is indicated.

Figure S2. H2A-H2B accumulation protects DNA from MNase digestion. Analyses of MNase digestion of A) a 621 bp 601 (601 x 3) DNA fragment capable of forming tri-nucleosomes, composed of three consecutive 207 bp Widom 601 nucleosome positioning sequences with linker DNA, and B) a 588 bp HTLV-1 LTR DNA fragment capable of forming mono-nucleosome. MNase digestion of naked DNA alone (first panels), DNA with H2A-H2B (second panels), chromatin (third panels), and chromatin with excess H2A-H2B (fourth panels).

Figure S3. The binding of excess H2A-H2B to the *GAL10* promoter does not grossly affect chromatin architecture, but does partially occlude MNase cleavage. A) Phosphor-image and quantitation of extension products from the *GAL1* promoter region and chromatin from wild type (green) or *nap1Δ* cells (red). This region of the *GAL* locus does not accumulate excess dimer when *NAP1* is deleted. B) Phosphor-image and quantitation of extension products from the *GAL10* promoter region and chromatin from wild type (green) or *nap1Δ* cells (red). This region of the *GAL* locus accumulates excess dimer when *NAP1* is deleted. Radio-labeled DNA size standards and lengths are shown to the left of each gel image. The location of the *GAL1* and *GAL10* TATA sequences and the MNase hyper-sensitive sites (HS) adjacent to the UAS are indicated to the right of each gel image. The + and ++ above the lanes correspond to, 16 or 32 $^{U}/_{ml}$ of MNase, respectively used to digest each sample.

Figure S4. Occupancy of the histone variant H2A.Z (Htz1) is unchanged in the *nap1Δ* strain. A) Occupancy of TAP tagged Htz1/H2A.Z at the *GAL* locus in the wild type (white bars) and nap1Δ (black bars) strain via chromatin-tandem affinity purification assay. Occupancy at each *GAL* location was normalized to occupancy at the telomere. Bars reflect the means of three biological replicates ± standard deviation; no significant differences were observed. B) Western blots of Htz1 levels in wild type (wt) and *nap1Δ* cells indicate no change in levels; TBP levels are shown as an internal control.

Figure S5. When induced, the *GAL* locus does not accumulate H2A-H2B in *nap1Δ*. A) Ratios of H2B to H3 occupancy at the *GAL* locus when cells are cultured in galactose (activated condition) show no differences between the wild type (white bars) and *nap1Δ* (black bars) strains. The histone occupancy of H2B and H3 were determined by ChIP assays and shown in Figure 4. B) Western blots of total histone levels in wt and *nap1Δ* cells cultured in galactose indicate no change in levels; TBP levels are shown as an internal control.

Figure S6. Doxycycline represses HA-tagged histone mRNA expression and does not affect *GAL* gene expression. The wild type and *nap1*Δ strains were cultured under transcriptionally repressed (glucose) or active (galactose) conditions. After the addition of doxycycline, cells were collected every hour for five hours. Total RNA was isolated from each sample and $^{HA}H2B$, *GAL7* and $tRNA^{W}$ transcripts were detected by S1 nuclease digestion using a ^{32}P-labeled probe specific to $^{HA}H2B$, *GAL7* or $tRNA^{W}$. The transcript level of the doxycycline-regulated HA-tagged histone diminishes within one hour of doxycycline treatment in both glucose and galactose media.

Figure S7. ^{HA}H2B protein level and chromatin occupancy at a telomere-proximal region decrease during treatment. The wild type strain containing both endogenous histone H2B and doxycycline-regulated histone ^{HA}H2B (plasmid-born, HA-tagged) was cultured under transcriptionally repressed conditions. Following addition of doxycycline (to turn off expression of ^{HA}H2B), cells were collected every hour for 5 hours, followed by immunoblotting to determine protein expression level and ChIP to determine occupancy. The HA-tagged histones represent less than 1% of the total (tagged and endogenous) histone expression levels (data not shown), therefore assays utilizing an anti-H2B antibody reflect primarily the endogenous protein. A) The protein levels of tagged histone ^{HA}H2B were detected using anti-HA antibody. B) The protein levels of endogenous histone H2B were detected using anti-H2B antibody. The occupancy of tagged histone ^{HA}H2B (C) and endogenous histone H2B (D) at a telomere proximal location during doxycycline treatment was determined by ChIP assay. The protein expression level and occupancy of the doxycycline-regulated histone ^{HA}H2B drops temporally following doxycycline treatment whereas the endogenous histone level and occupancy does not. Data in (A)-(D) reflect the mean from 3 biological replicates ± standard deviation.

Figure S8. The cellular protein levels of epitopically expressed HA-tagged histones and endogenous histones are not affected by the deletion of Nap1. The wild type strain (shown in white) and the *nap1*Δ strain (shown in black), both containing endogenous histones and the plasmid expressing doxycycline-regulated HA-tagged histone (^{HA}H2B or H3^{HA}), were cultured under transcriptionally repressed conditions (glucose). Following addition of doxycycline (to turn off the expression of ^{HA}H2B or H3^{HA}), cells were collected every hour for 5 hours, followed by immunoblotting. The HA-tagged histones represent less than 1% of the total (tagged and endogenous) histone

expression levels (data not shown), therefore assays utilizing an anti-H2B or anti-H3 antibody reflect primarily the endogenous protein. The protein expression levels of ^{HA}H2B (A) and H3^{HA} (B) were detected with anti-HA antibody. The protein expression levels of the total/endogenous H2B (C) and H3 (D) were detected with anti-H2B and anti-H3 antibodies, respectively. The protein expression level (for HA-tagged or endogenous histones) at T_0 in each strain was set as 100. Bars reflect the means of three biological replicates ± standard deviation.

Figure S9. DNA sequence affects nucleosome formation and stability. Nucleosome reconstitutions with 601, and the indicated *GAL* fragments. Increasing molar amounts of histone octamer were incubated with the indicated DNA fragments, complexes were resolved in 5% native gels and DNA visualized by ethidium bromide staining.

Figure S10. Hexasome and nucleosome formation is dependent upon DNA sequences. In the nucleosome reconstitution with histone octamer and DNA fragments using salt dilution method (as shown in Supplemental Figure 9) multiple forms of DNA-histone complexes were detected. To identify the complexes, nucleosome reconstitution was performed with fluorescently labeled histones. The Alexa488 labeled H2B is shown in green and Atto647N labeled H4 in red. Therefore, the canonical nucleosome with equal molar of H2B and H4 would be visualized in yellow and the hexasome with H2B to H4 ratio as 1:2 would be in orange. Representative gels of 601, the *GAL10* promoter (GAL10PRO) and *GAL1* promoter (GAL1PRO) are shown. Based on the color and intensity, we conclude both hexasome and nucleosome are formed on 601 and GAL10PRO. In contrast GAL1PRO forms predominantly nucleosomes.

Figure S11. Hexasomes and nucleosomes are stably position on the DNA sequences. It is possible that the multiple forms of DNA-histone complexes could be differently positioned nucleosomes. To test this, we incubated the reconstituted nucleosomes under different conditions, such as heat shift at 42°C, lower salt concentration (from 300 mM to 50 mM) or both, which would serve to disrupt non-positioned histone-DNA complexes. Representative gels for GAL7 promoter and ORF are shown. The results indicate that the pattern of DNA-histone complex bands does not change under these conditions, supporting the conclusion that these are stably positioned DNA-histone complexes.

Figure S12. Nap1 plays multiple roles in histone dynamics in vivo. See text for details.